Yang Zou, Xin Na, Yimiao Sun, Yande Chen, Yuan He *Tsinghua University, Beijing, China*

Photo, istockphoto.com

Backscatter Meets Audio: A Step Toward RF Computing

Excerpted from "Satori: In-band Analog Backscatter for Audio Transmission," from *MobiSys '25: Proceedings of the 23rd Annual International Conference on Mobile Systems, Applications and Services*, with permission. https://dl.acm.org/doi/10.1145/3711875.3729153 ©ACM 2025

Passive Internet of Things (Passive IoT) has attracted widespread attention from both academia and industry due to its potential for ubiquitous deployment and round-the-clock operation without the need for dedicated power sources [1]. As a key enabling technology for Passive IoT, backscatter communication has been an active research area for over a decade and has achieved remarkable progress [2, 3, 4]. We have witnessed the feasibility of implementing backscatter communication using various ambient energy sources [5, 6, 7, 8], with the communication range continuously extending from a few meters to reliably transmitting data over distances of more than one kilometer [9].

Despite the above progress, two critical challenges remain that hinder the technology's effectiveness, particularly in typical application scenarios, such as audio sensing in industrial environments.

- First, achieving high audio fidelity requires the entire digital front-end, including analog-to-digital conversion and real-time signal processing, to operate continuously at high speed, which leads to substantial power consumption.
- Second, to avoid interference from the strong excitation signal, most existing designs shift the backscattered signal to a different frequency band, necessitating a fast and power-hungry frequency-shifting clock.

Inspired by the concept of RF computing [10], our recent research has made significant progress in addressing the above challenges. We propose *Satori*, the first in-band analog backscatter system designed for audio transmission. As illustrated in Figure 1, the Satori tag backscatters the ambient Wi-Fi signals in industrial environments and transmits audio through in-band analog modulation. Satori introduces two key innovations to enable low-power, high-fidelity audio sensing:

- Methodologically, Satori redefines the traditional sensing pipeline: instead of digitizing the audio signal first, it performs analog modulation by directly mapping the analog audio signals onto the reflected phase in the analog domain, thereby significantly reducing real-time digital signal processing and its associated power consumption.
- Technically, Satori enables in-band audio transmission by embedding the audio signal directly within the spectrum of the ambient Wi-Fi excitation, eliminating the need for a power-intensive frequency-shifting mechanism.

By leveraging analog modulation and in-band transmission, Satori achieves ultra-low-power audio transmission. It consumes only about 20 microwatts for its modulation, supports a sampling rate above 40 kHz, and achieves an SNR exceeding 18 dB, making it well-suited for energy-constrained, high-fidelity audio sensing applications.

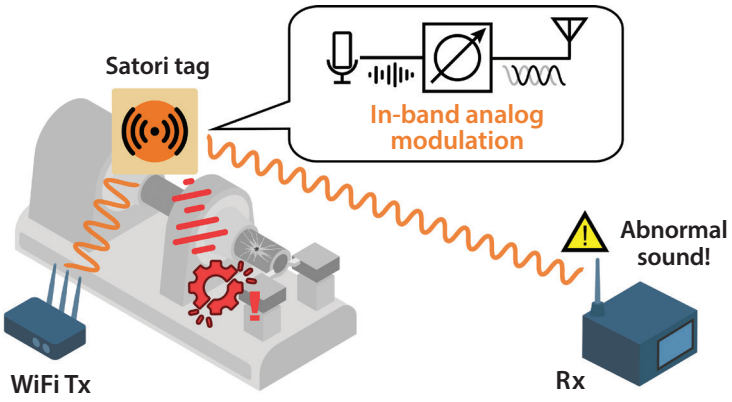

FIGURE 1. Audio sensing applications enabled by Satori.

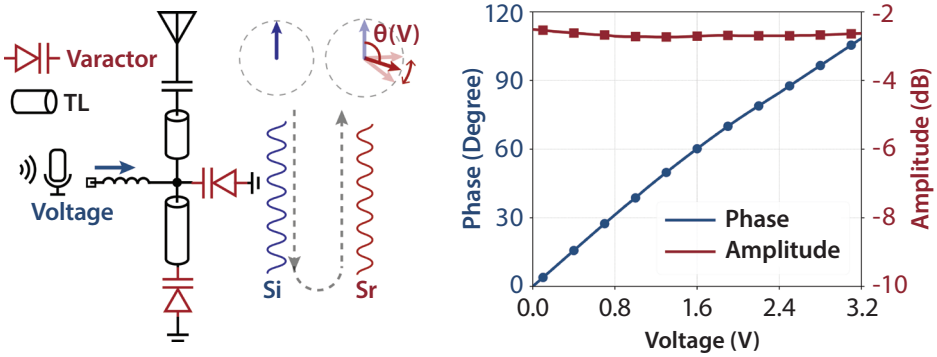

(a) schematic

(b) phase and amplitude response

FIGURE 2. The schematic and performance of the phase shifter.

DESIGN

Overview

The primary design goal of Satori is to enable high-fidelity and interference-resilient analog audio embedding on a power-constrained backscatter tag. To achieve this, Satori introduces two core components:

- The precise RF phase shifter: it serves as an analog-domain computing primitive directly maps continuous audio signals from a low-power microphone into a finely controlled reflection phase. We carefully design its structure to produce a significant change in reflection phase even with small variations in audio voltage, enabling both accurate phase embedding and robustness against noise.
- The in-band analog modulation scheme: it encodes the audio voltage into the shape of a triangle formed by three backscattered Wi-Fi symbols in the IQ plane. Since self-interference typically introduces an identical offset across consecutive Wi-Fi symbols, it does not alter the shape of the triangle embedded by the tag, thereby enabling robust audio embedding despite strong in-band interference.

We also design a corresponding receiver algorithm that addresses challenges, such as carrier frequency offset (CFO) and deep channel fading, enabling high-quality recovery of the audio signal.

Precise RF Phase Embedding

The core of Satori's RF-domain voltage-to-phase computation is a carefully designed analog phase shifter. It takes input from an ultra-low-power microphone and dynamically adjusts its reflection phase in real time according to the input voltage. To enable accurate and robust voltage-to-phase mapping on a low-power backscatter tag, this phase shifter must satisfy the following specifications:

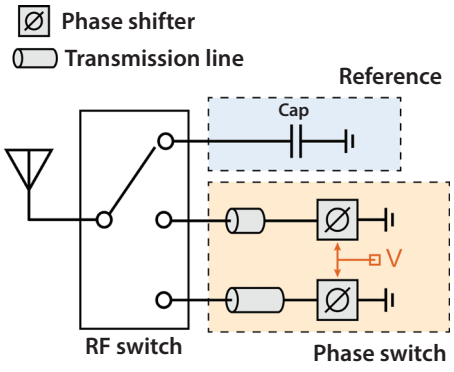

FIGURE 3. Satori's modulation circuit.

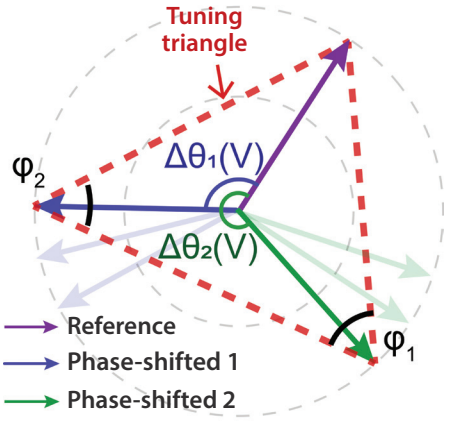

FIGURE 4. The modulation scheme.

- **Ultra-low computing power consumption:** The phase shifter must operate with minimal power overhead to remain compatible with the tag's microwatt-level power budget.
- **Wide-range linear voltage-to-phase response:** The phase shifter must produce a sufficiently large phase shift in response to small voltage variations across its entire input range, ensuring robustness against noise.
- **Flat phase response across the entire Wi-Fi band:** The phase shift applied must be consistent across the whole Wi-Fi band to avoid frequency-dependent distortion.

Changing the reflected phase of the backscatter tag fundamentally involves controlling the impedance at the terminal of the antenna. In an RF circuit, the reflected phase is determined by the terminal loads reactance jX_L and the impedance of the antenna Z_0 as:

$$\theta_{reflect} = \angle\left(\frac{Z_0 - jX_L}{Z_0 + jX_L}\right)$$

Therefore, the core of our design lies in constructing a terminal load with reactance that can vary continuously and in real time with audio signals. To achieve this, we consider a varactor diode. Under reverse bias, the junction capacitance of a varactor diode changes in accordance with the bias voltage. Furthermore, since it operates in reverse bias, its static current is only several picoamperes, resulting in negligible power consumption. These make the varactor an ideal component for achieving analog computing under a sub-microwatt power budget. In the Satori tag, we directly use the voltage output from a low-power microphone as the reverse bias voltage applied to the varactor diode, thereby enabling the direct conversion of audio signals into reflected phase.

However, a single varactor diode exhibits an inherent nonlinearity: its capacitance-voltage sensitivity (dC/dV) decreases as the reverse bias voltage increases. When the microphone outputs a high voltage, the variation in reflection phase becomes extremely small, making the audio details prone to being overwhelmed by the noise. To address this critical issue, we adopt a dual-varactor compensation architecture. As shown in Figure 2a, a second varactor diode is introduced in parallel and coupled via a transmission line (TL). The core idea of this design is to exploit the second varactor to compensate for the nonlinear characteristics of the first varactor. By optimizing the characteristic impedance of the TLs between the two varactors, we achieve a reflection phase response with a high and flat phase-voltage slope across the entire operating voltage range. As shown in Figure 2b, the phase shifter exhibits a wide and linear voltage-phase response, with the attenuation maintained at approximately 2 dB. This ensures high sensitivity for phase modulation regardless of the output voltage, thereby preserving the fine details of the audio signal.

To ensure a flat phase response across the entire 20 MHz Wi-Fi channel bandwidth, we minimized the length of transmission lines while maintaining optimal phase shift performance, thereby reducing phase distortion caused by propagation delay. Measurement results show that within the 20 MHz bandwidth, the maximum phase deviation introduced by the shifter is only 0.49 degrees, corresponding to an error of less than 0.5%.

Despite operating with extremely limited resources, Satori enables high-performance IoT applications, showcasing the potential of efficient analog-domain processing

Through these three key technologies, we develop a high-performance analog phase shifter. This shifter enables precise and linear mapping of analog audio voltage to the phase of the reflected signal, establishing a robust hardware foundation for the analog computation.

In-band Analog Modulation

To achieve high-quality in-band audio backscattering, the modulation scheme must satisfy two core requirements:

- It must reliably embed analog audio information in the presence of self-interference that is much stronger than the backscattered signal.
- The modulation rate must be sufficiently high to support the tens of kHz sampling rates required for high-fidelity audio.

The key insight lies in the slow-varying nature of self-interference: the received signal is the sum of the direct-path self-interference and the backscattered signal. Since the direct-path channel varies slowly, the self-interference vector remains nearly

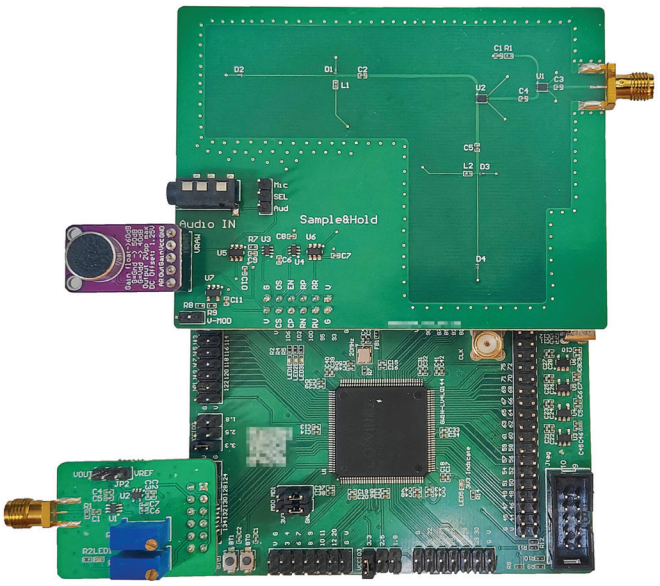

FIGURE 5. The PCB prototype of the Satori tag.

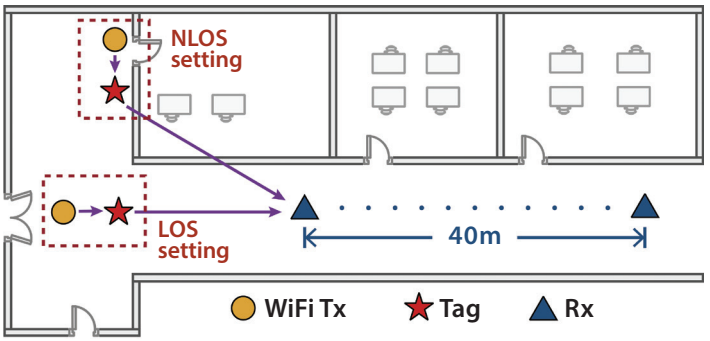

FIGURE 6. The experiment setup.

constant in several consecutive symbols. This means that although self-interference distorts the absolute phase of the symbols, it causes nearly consistent offset across consecutive symbols. If the tag applies reflection phases related to the current audio voltage but differing across symbols, the audio information can be stably embedded in the relative geometric relationships among these symbols in the IQ plane.

To achieve this, we design the Satori tag's modulation circuit shown in Figure 3, which consists of a radio-frequency switch and three termination loads: one fixed capacitor and two analog phase shifters. When the tag detects a Wi-Fi packet arriving, it uses the RF switch to sequentially connect the antenna to these three loads across three consecutive Wi-Fi symbol periods. This first generates a reference symbol with a fixed reflection phase and two phase-shifted symbols, whose reflection phases are controlled by the audio voltage *V*. As shown in Figure 4, the three modulated symbols produce three complex vectors in the IQ domain. These points form a triangle, referred as the tuning triangle. The two internal angles φ_1 and φ_2 of this triangle are directly determined by the phase shifts $\Delta\theta_1(V)$ and $\Delta\theta_2(V)$ of the two modulated symbols as:

$$\varphi_1 = \frac{1}{2}\Delta\theta_1(V),\ \varphi_2 = \frac{1}{2}(2\pi - \Delta\theta_2(V))$$

Consequently, the audio voltage is fully embedded in the geometric shape of the triangle. In practical in-band transmission, the self-interference vector only translates the entire tuning triangle in the IQ plane without altering its shape or internal angles. The receiver can accurately decode the embedded audio voltage by analyzing the triangle's intrinsic geometric features.

Furthermore, thanks to the efficient three-symbol encoding scheme, Satori achieves an equivalent audio sampling frequency exceeding 40 kHz, meeting the requirements for high-fidelity audio transmission.

Audio Signal Recovery

At the receiver, the key to recovering audio from the Wi-Fi signal in Satori lies in extracting the tuning triangle embedded by the tag within the Wi-Fi OFDM symbols. To achieve this, we focus on the pilot subcarriers of each Wi-Fi symbol, which are fixed and known across all symbols. Specifically, the receiver first performs standard Wi-Fi baseband processing to recover the OFDM symbols. Subsequently, the pilot subcarriers of each symbol are extracted. Three Wi-Fi symbols' pilot subcarriers form a triangle in the IQ plane, representing the embedded tuning triangle. By computing the internal angle of this triangle, the system can accurately reconstruct the original analog audio voltage.

However, in practical receivers, CFO introduces a time-accumulating common phase rotation across all symbols, severely distorting the shape of the tuning triangle and rendering it unidentifiable. To address this, we propose a lightweight two-step CFO calibration scheme. In the first step, we perform linear fitting on the phase of the reference symbol, which should remain fixed, to achieve a coarse estimation and removal of the CFO. In the second step, we measure the phase difference between the cyclic prefix (CP) and the last 16 samples of each Wi-Fi symbol, enabling fine-grained correction of the CFO.

Moreover, frequency-selective fading causes large power variations across pilot subcarriers, potentially burying the tuning triangle in noise on some subcarriers. To improve robustness, we implement a fade-adaptive audio recovery method. We first recover audio independently on each pilot subcarrier. Then, we analyze geometric features of the triangle, such as the distance from each vertex to the centroid, to assess the fading on each subcarrier. Based on this assessment, we assign adaptive weights to the audio estimates and compute the final audio signal via weighted averaging. These processes enable Satori to reliably reconstruct high-quality audio even in challenging wireless environments.

IMPLEMENTATION

Figure 5 shows the prototype of Satori on a four-layer PCB with COTS components. It mainly consists of an RF front end and a logic controller. The RF front end includes the analog modulation circuit and the packet detection circuit for synchronizing with Wi-Fi symbols. For the analog modulation circuit, we employ the MAVR-000120

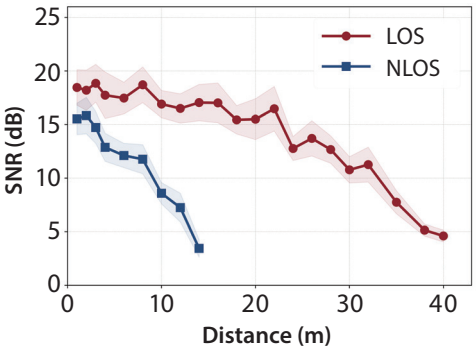

FIGURE 7. The SNR vs. Tag-Rx distance.

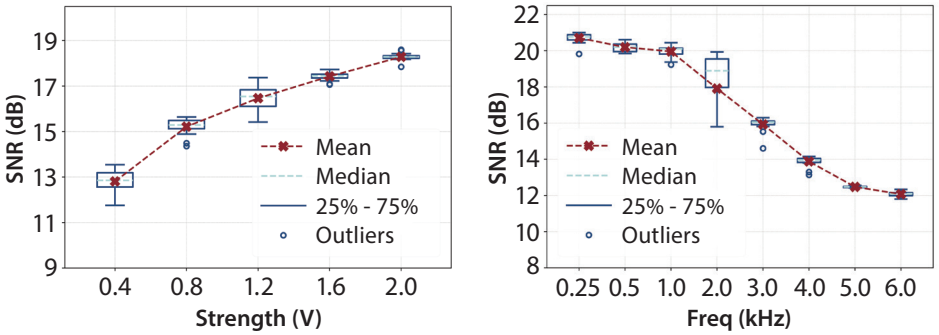

(a) The SNR vs. strength

(b) The SNR vs. frequency

FIGURE 8. The SNR under varying audio strength and frequency.

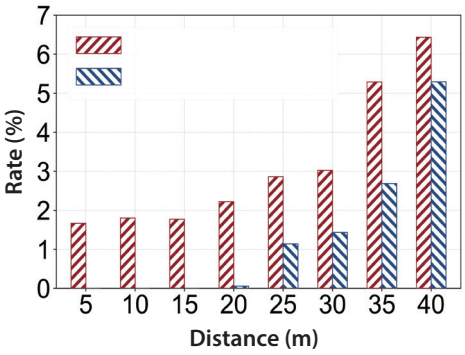

(a) Industrial fault diagnosis

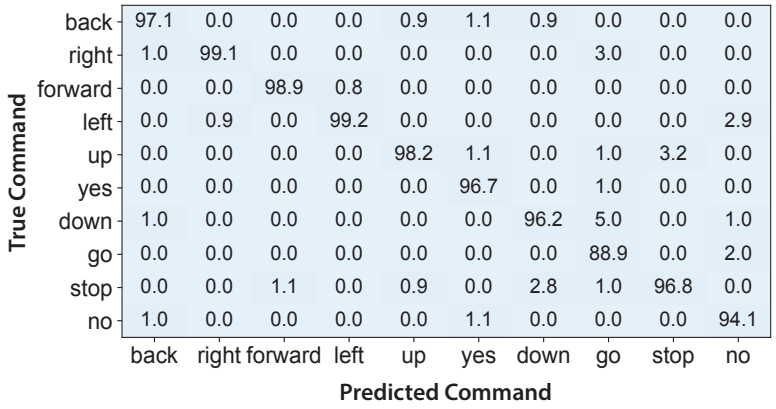

(b) Voice command recognition

FIGURE 9. Satori's performance in acoustic intelligence applications.

varactor diode to construct the phase shifter, which operates under reverse bias with a bias current as low as 1.6 pA. The SKY13335 RF switch is selected for its low insertion loss (typical 0.4 dB@2.4 GHz) and low power consumption. The total power consumption of the two switches is only 20 uW. The packet detection circuit is built around the LT5534 envelope detector and the TLV3201 comparator, which detects the arrival of Wi-Fi packets and triggers the tag's modulation.

The control unit uses a low-power GW1N-LV4 FPGA. Its function only includes timing control without any signal processing. With custom ASIC design, the power consumption can be reduced to approximately 2 microwatts.

For the transceiver setup, we use the USRP N210 as the Wi-Fi transmitter, operating at a power level of 20 dBm to emit IEEE 802.11n signals. The receiver employs the USRP B210 to capture raw IQ data, which is subsequently processed by our audio recovery algorithm in MATLAB. For more details, refer to the full paper in Mobisys 2025 [11].

EVALUATION

We evaluate Satori in an indoor corridor environment, as illustrated in Figure 6, and measure the SNR of the audio signal recovered by Rx. As shown in Figure 7, in the LOS scenario, Satori achieves an audio SNR exceeding 18 dB at a tag-to-receiver (Tag-Rx) distance of 8 m, and maintains an SNR above 10 dB up to 32 m. Even in the challenging NLOS scenario, Satori sustains a 12 dB SNR at 8 m, demonstrating its robustness in complex industrial or home environments.

To comprehensively characterize system performance, we further examine its behavior under varying audio characteristics. The results are shown in Figure 8. Regarding audio amplitude, when the microphone output voltage ranges from 0.4 V to 2.0 V (a dynamic range of 14 dB), the recovered audio SNR degrades by only approximately 6 dB. For audio frequency, the system maintains SNR above 15 dB across 200 Hz to 4 kHz and achieves an SNR exceeding 10 dB even at 6 kHz, which is sufficient to cover the critical frequency bands of human speech and most industrial equipment.

We further employ the audio transmitted by Satori directly for end-to-end intelligent tasks, including industrial fault diagnosis and voice command recognition. In fault diagnosis, Satori achieves an average error rate of about 5% at a Tag-Rx distance of 35 m, as shown in Figure 9a. For voice command recognition, the system attains an average accuracy above 95% across 10 command classes at a 20 m Tag-Rx distance, with the lowest accuracy still approaching 88%, as shown in Figure 9b. These results demonstrate that the audio transmitted by Satori is of sufficient quality to support diverse acoustic intelligence applications.

CONCLUSION AND FUTURE WORK

Satori achieves low-power, high-fidelity audio sensing. Its innovative design reflects the core principle of RF computing: using novel specialized RF circuits to perform computation directly in the analog domain, thus avoiding the complexity and energy costs of traditional digital signal processing. Despite operating with extremely limited resources, Satori enables high-performance IoT applications, showcasing the potential of efficient analog-domain processing. We believe Satori not only marks a significant step forward in backscatter technology, but also stimulates further research and application exploration in the field of RF computing. ■

Yang Zou is currently a PhD student at Tsinghua University. He received his BE degree from the Beijing University of Aeronautics and Astronautics (BUAA). His research interests include wireless networks and communication.

Xin Na is currently a PhD student at Tsinghua University. He received his BE degree from Tsinghua University. His research interests include wireless networks and low-power IoT.

Yimiao Sun is currently a PhD student at Tsinghua University. He received his BE degree from the University of Electronic Science and Technology of China (UESTC). His research interests include mobile computing and wireless sensing.

Yande Chen is currently a PhD student at Tsinghua University. He received the BE degree in the School of Software from Tsinghua University. His research interests include Internet of things and wireless sensing.

Yuan He is a professor in the School of Software and BNRist of Tsinghua University. He received his PhD from Hong Kong University of Science and Technology. His research interests include Internet of Things, wireless networks, mobile and ubiquitous computing.

REFERENCES

[1] 3GPP. 2025. 3GPP Radio Access Networks Work Group 1. https://www.3gpp.org/3gpp-groups/radio-access-networks-ran/ran-wg1.

[2] Vincent Liu, Aaron Parks, Vamsi Talla, Shyamnath Gollakota, David Wetherall, and Joshua R. Smith. 2013. Ambient backscatter: Wireless communication out of thin air. *ACM SIGCOMM Computer Communication Review.*

[3] Renjie Zhao, Fengyuan Zhu, Yuda Feng, Siyuan Peng, Xiaohua Tian, Hui Yu, Xinbing Wang. 2019. OFDMA-Enabled Wi-Fi Backscatter. Proceedings of the ACM MobiCom.

[4] Jia Zhao, Wei Gong, and Jiangchuan Liu. 2021. Microphone array backscatter: An application-driven design for lightweight spatial sound recording over the air. *Proceedings of the ACM MobiCom*.

[5] Zicheng Chi, Xin Liu, Wei Wang, Yao Yao, and Ting Zhu. 2020. Leveraging ambient LTE traffic for ubiquitous passive communication. *Proceedings of the ACM SIGCOMM*.

[6] Anran Wang, Vikram Iyer, Vamsi Talla, Joshua R. Smith, and Shyamnath Gollakota. 2017. FM backscatter: Enabling connected cities and smart fabrics. *Proceedings of the USENIX NSDI*.

[7] Pengyu Zhang, Dinesh Bharadia, Kiran Joshi, and Sachin Katti. 2016. Hitchhike: Practical backscatter using commodity WiFi. *Proceedings of the ACM SenSys*.

[8] Maolin Zhang, Si Chen, Jia Zhao, and Wei Gong. 2021. Commodity-level BLE backscatter. *Proceedings of the ACM Mobisys.*

[9] Yao Peng, Longfei Shangguan, Yue Hu, Yujie Qian, Xianshang Lin, Xiaojiang Chen, Dingyi Fang, and Kyle Jamieson. 2018. PLoRa: A passive long-range data network from ambient LoRa transmissions. *Proceedings of the ACM SIGCOMM.*

[10] Yuan He, Yimiao Sun, Xiuzhen Guo. 2025. RF computing: A new realm of IoT research. *Springer Journal of Computer Science and Technology.*

[11] Yang Zou, Xin Na, Yimiao Sun, Yande Chen, Yuan He. 2025. Satori: In-band analog backscatter for audio transmission. *Proceedings of the ACM Mobisys.*

Photo, istockphoto.com